SEISMIC SOIL PRESSURES AGAINST VERTICAL RIGID WALLS

Guoxi Wu[1], Ph.D.

ABSTRACT

Approximate analytical solutions are presented for evaluating dynamic soil pressures against a vertical rigid wall retaining a uniform viscoelastic soil medium of finite length subjected to base excitations. The accuracy of the approximate solutions has been verified using Wood's rigorous solutions. The finite element method of analysis has been used for analysis of non-uniform viscoelastic layered soil medium. Peak dynamic thrusts and heights of the resultant forces have been obtained for three types of soil profiles under earthquake loads using ten preselected accelerograms. For each type of soil profile, 250 combinations of accelerogram and shear modulus G are examined in order to construct the envelopes of peak dynamic thrust. The results are presented as functions of nondimensional frequency ratio ω/ω_{11}. Possible ranges of dynamic thrusts are recommended for use in the seismic design of rigid walls.

INTRODUCTION

For seismic design of a rigid wall it is important to know the magnitude and distribution of seismic pressure on the wall induced by earthquake motion. Probably the earliest researches dealing with seismic induced earth pressure on retaining structures were those of Mononobe (1929) and Okabe (1926). The Mononobe-Okabe method is the modification of Coulomb's classic earth pressure theory which takes into account the inertia forces caused by earthquake accelerations. Seed and Whitman (1970) made a detailed evaluation of the Mononobe-Okabe method. One of the basic requirements of applying the Mononobe -Okabe method is that the wall has to move sufficiently to create a limit equilibrium state in the backfill. This condition is not satisfied in most rigid wall cases.

Several researchers have used elastic wave theory to derive seismic soil pressure against a rigid wall. Matuo and Ohara (1960) obtained an approximate elastic solution for the dynamic soil pressure on a rigid wall using a two-dimensional analytical model. They simplified the problem by assuming zero vertical displacement in the soil mass. This simplification leads to infinitely large wall pressure when Poisson's ratio of the soil is equal to 0.5 as in a fully saturated undrained backfill. Scott (1973) used a one-dimensional elastic shear beam connected to the wall by Winkler springs to model the problem. Recent work by Veletsos and Younan (1994) concluded that Scott's model does not adequately describe the action of the system and may lead to large errors.

Wood (1973) provided analytical solutions for the response of a rigid wall retaining a soil

[1] AGRA EARTH & ENVIRONMENTAL LTD.
2227 Douglas Road, Burnaby, B.C., V5C 5A9

backfill of finite length subjected to base excitation. His work is considered to be one of the more important contributions to understanding of this problem. However Wood's solution is mathematically too complicated to apply in engineering practice even under very idealistic conditions of a homogeneous soil layer under harmonic loading. Veletsos and Younan (1994) presented analytical solutions of the response of semi-infinite, uniform viscoelastic soil medium subjected to base excitations. Their model with $\sigma_y=0$ approximation works well for a wall with a semi-infinite backfill, but it overestimates significantly the soil pressures for a more confined backfill. Details of the comparison is given in a later section.

The primary objective of this paper is to develop a simple but reliable method for computing the dynamic soil pressures against rigid walls with backfills of finite length. The method is then used to construct envelopes of peak dynamic thrust for three soil profiles subjected to earthquake excitations.

ANALYTICAL SOLUTIONS FOR HOMOGENEOUS SOIL BACKFILLS

Analytical Approximation of the Problem

Figure 1(a) shows the geometry of the problem and its boundary conditions. A uniform elastic soil medium is confined by two vertical rigid walls at its two side boundaries and a rigid base. The soil layer has a total length of 2L and a height of H. Subjected to horizontal seismic body force, the soil medium in the system generates an antisymmetric field of horizontal normal stresses σ_x with zero stresses $\sigma_x=0$ at $x = L$. Therefore the original wall-soil problem is equivalently represented by half of its geometry using this antisymmetric condition as shown in Figure 1(b).

The soil is assumed to be a homogeneous, isotropic, visco-elastic solid with a mass density ρ, a shear modulus G and Poisson's ratio μ. Damping of soil is modelled by applying equivalent viscous damping to the wall-soil system.

For the system investigated, the vertical motions and stresses are considered not to have significant effects on the resulting wall pressures and forces as they will be demonstrated later in the paper. Therefore only the horizontal displacement u in the X direction is modelled in the analysis. Using the 1-D shear beam analogy, subjected to a base acceleration $\ddot{u}_b(t)$, the governing equation of the undamped forced vibration of the backfill in the horizontal direction can be written as

$$G\frac{\partial^2 u}{\partial^2 y} + \theta\, G\frac{\partial^2 u}{\partial^2 x} - \rho\frac{\partial^2 u}{\partial^2 t} = \rho\ddot{u}_b(t) \qquad (1)$$

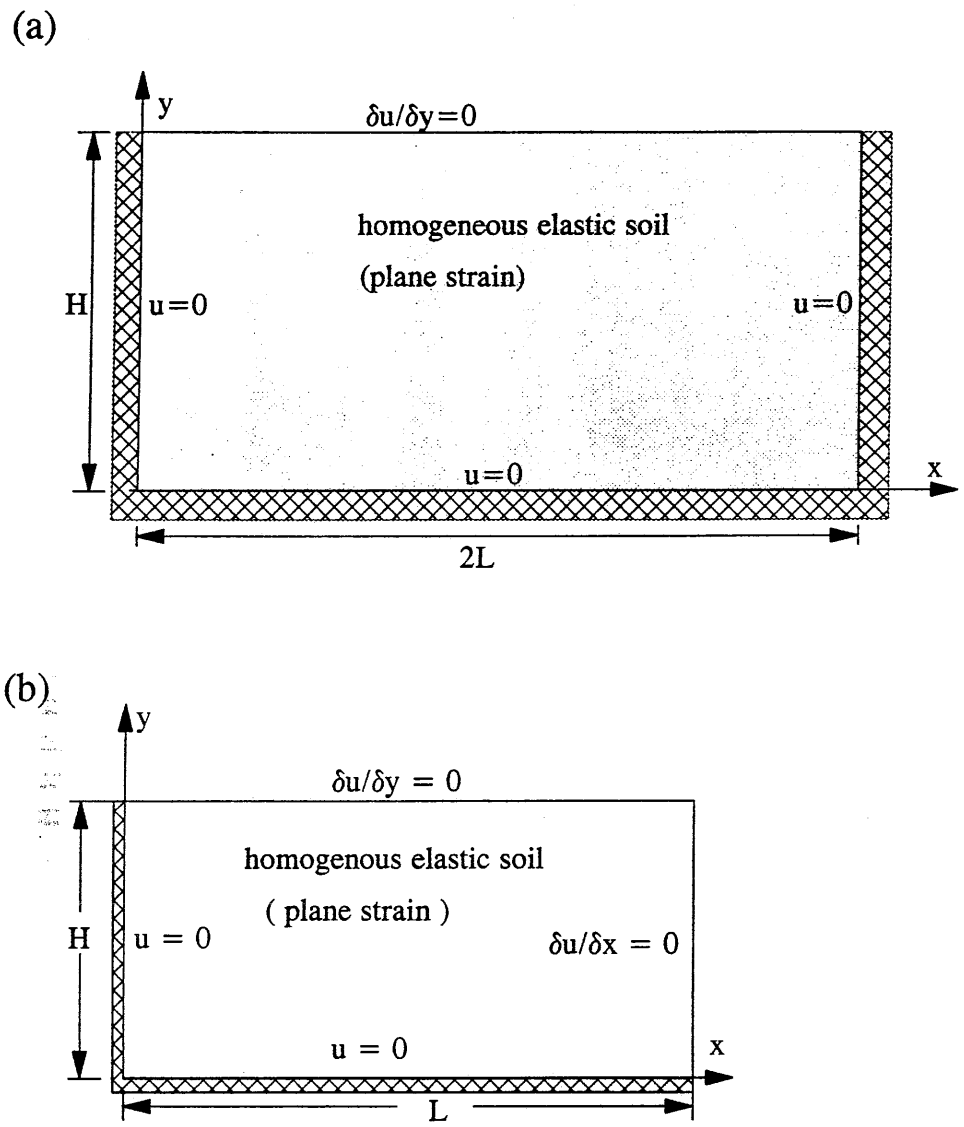

Fig. 1 Definition of rigid-wall problem (a) original problem (b) equivalent problem by using antisymmetric condition

and the normal stress in the x direction σ_x is given by

$$\sigma_x = \beta\ G\ \frac{\partial u}{\partial x} \qquad (2)$$

where t is time, θ and β are functions of Poisson's ratio μ.

The first term on the left-hand side in equation (1) reflects the horizontal shear stress contribution of a one-dimensional shear beam, and the second term includes the contribution of the normal stress σ_x due to the existence of the wall. The precise expressions for θ and β depend on the approximations used to model the wall-soil system. Three forms of approximation are examined and their corresponding expressions for θ and β are given below (Wu, 1994).

(i). v = 0 approximation (Matuo and Ohara, 1960). In this case, the displacements in the vertical direction Y are assumed to be zero. It is found that

$$\theta = \beta = \frac{2(1-\mu)}{1-2\mu} \qquad (3)$$

(ii). σ_y =0 assumption (Veletsos and Younan, 1994). In this case, the normal stresses in the vertical direction Y are assumed to be zero. It is found that

$$\theta = \frac{2-\mu}{1-\mu} \qquad (4)$$

$$\beta = \frac{2}{1-\mu} \qquad (5)$$

(iii). the proposed model. In this case, the stress coefficient β in Eq.(2) is determined first using the $\sigma_y = 0$ approximation, and the coefficient θ in Eq.(1) is then obtained assuming that the shear stress can be modelled using the shear beam analogy, i.e., $\tau_{xy} = G^*\partial u/\partial y$. It is found that

$$\theta = \beta = \frac{2}{1-\mu} \qquad (6)$$

The v = 0 approximation in (i) results in infinitely large normal stress σ_x as the Poisson's ratio μ approaches 0.5. The $\sigma_y = 0$ approximation in (ii) works well for a wall retaining semi-infinite backfill, e.g., L/H=5.0, as shown by Veletsos and Younan (1994). But this approximation results in significant overestimate of soil pressure against a wall retaining a more confined backfill, e.g., L/H=1.5, as demonstrated in this paper. The proposed model in (iii) works well for both cases with L/H=5.0 and L/H=1.5. The results obtained using the proposed model (iii) are presented herein although the derivation of solutions retains the use of both coefficients θ and β.

Solutions of the Problem

Equation (1) is solved subject to the following boundary conditions:

(1). $u = 0$ at $y=0$
(2). $u = 0$ at $x=0$
(3). $\partial u/\partial x=0$ at $x=L$
(4). $\partial u/\partial y=0$ at $y=H$

The angular natural frequencies of the wall-soil system are found to be

$$\omega_{mn} = \sqrt{\frac{G}{\rho}\ (b_n^2 + \theta a_m^2)} \qquad (7)$$

where

$$a_m = \frac{(2m-1)\,\pi}{2L} \qquad m = 1,2,3,.... \qquad (8)$$

$$b_n = \frac{(2n-1)\,\pi}{2H} \qquad n = 1,2,3,.... \qquad (9)$$

The fundamental frequency ω_{11} corresponding to m=1 and n=1 is

$$\omega_{11} = \frac{\pi}{2H}\sqrt{\frac{G}{\rho}} \cdot \sqrt{1+\theta\frac{H^2}{L^2}} \qquad (10)$$

Using the method of separation of variables, the transient displacement variable u(x,y,t) in equation (1) is found to be

$$u(x,y,t) = \sum_{m=1}^{\infty}\sum_{n=1}^{\infty} \sin(a_m x)\cdot\sin(b_n y)\cdot\alpha_{mn}\cdot f_{mn}(t) \qquad (11)$$

where $f_{mn}(t)$=transient modal solution corresponding to a particular modal angular frequency ω_{mn}

α_{mn} = mode-participation factor and

$$\alpha_{mn} = \frac{16}{(2m-1)\,(2n-1)\,\pi^2} \qquad (12)$$

Viscous damping of the wall-soil system is incorporated by using a modal damping ratio λ for

each mode. In the case of a damped forced vibration, the transient modal solution $f_{mn}(t)$ is obtained from the following equation

$$\ddot{f}_{mn}(t) + 2\lambda\omega_{mn}\cdot\dot{f}_{mn}(t) + \omega_{mn}^2\cdot f_{mn}(t) = -\ddot{u}_b(t) \qquad (13)$$

Therefore it is seen from Eq.(13) that $f_{mn}(t)$ is the relative displacement solution of a single degree of freedom system of an angular frequency ω_{mn} and a damping ratio λ subjected to a base acceleration $\ddot{u}_b(t)$.

Dynamic Soil Pressures

The dynamic soil pressure acting on the wall is determined from the horizontal normal stress σ_x at x=0. The dynamic pressure distribution along the wall is

$$p(t) = \sigma_x(x,y,t)_{x=0} = \beta G\frac{\partial u}{\partial x}\Big|_{x=0} = \beta G\sum_{m=1}^{\infty}\sum_{n=1}^{\infty} a_m\alpha_{mn}\cdot\sin(b_n y)\cdot f_{mn}(t) \qquad (14)$$

The total dynamic thrust acting on the wall is then given by integration of soil pressure over the height of the wall

$$Q(t) = \int_0^H p(t)\cdot dy = \beta G\sum_{m=1}^{\infty}\sum_{n=1}^{\infty}\frac{a_m\alpha_{mn}}{b_n}\cdot f_{mn}(t) \qquad (15)$$

or

$$Q(t) = \beta G\sum_{m=1}^{\infty}\sum_{n=1}^{\infty}\frac{16 f_{mn}(t)}{\pi^2(2n-1)^2 L/H} \qquad (16)$$

The overturning dynamic moment acting at the base of the wall is

$$M_b(t) = \int_0^H y\cdot p(t)\cdot dy \qquad (17)$$

$$M_b(t) = \beta G\sum_{m=1}^{\infty}\sum_{n=1}^{\infty}\frac{a_m\alpha_{mn}\sin(b_n H)}{b_n^2}\cdot f_{mn}(t) \qquad (18)$$

For a harmonic base acceleration $\ddot{u}_b(t)=A_{max}\,e^{i\omega t}$, the steady-state response $f_{mn}(t)$ is found from Eq.(13) to be

$$f_{mn}(t) = -\frac{A_{max}}{(\omega_{mn}^2-\omega^2)+2i\cdot\lambda\omega_{mn}\cdot\omega}\cdot e^{i\omega t} \qquad (19)$$

For an earthquake excitation, the peak dynamic thrust Q^{mn} corresponding to the modal angular frequency ω_{mn} is obtained from the pseudo-spectral velocity $S_{mn}{}^{v}$ as

$$Q^{mn} = \beta G\cdot \frac{16}{\pi^2(2n-1)^2 L/H}\ \frac{S_{mn}^{v}}{\omega_{mn}} \qquad (20)$$

where $S_{mn}{}^{v} = \omega_{mn}\, S_{mn}{}^{d}$

$S_{mn}{}^{d}$ = response spectral displacement or the peak value of $f_{mn}(t)$ in Eq. (13).

STATIC SOLUTION AND MODEL VERIFICATION

Static Solution The static solution is obtained by applying a uniform horizontal body force of constant intensity $\ddot{u}_b(t) = A_{max}$ with time t. The static solution is the limit of dynamic solution when the period of the harmonic base excitation $\ddot{u}_b(t) = A_{max}\, e^{i\omega t}$ becomes infinitely large. The static thrust per unit length of the wall is determined as

$$Q^{st} = \beta G\ \frac{16A_{max}}{\pi^2 L/H}\ \sum_{m=1}^{\infty}\sum_{n=1}^{\infty}\ \frac{1}{(2n-1)^2\omega_{mn}} \qquad (21)$$

Model Verification

The approximate solutions are used to obtain the static force for two wall-soil systems: one with a semi-infinite backfill and the other one with a finite backfill. The semi-infinite backfill is approximated by using L/H=5.0 and the finite backfill is represented by using L/H=1.5.

The accuracy of the three approximate models namely, v = 0 approximation, σ_y= 0 approximation and the proposed model, is examined against Wood's rigorous solution (Wood, 1973) for both systems of L/H = 5.0 and L/H = 1.5. Wood's solution is strictly valid for both wall-soil systems under the condition that the interface between the soil and the wall is smooth and frictionless. Results of comparison are shown in Figure 2(a) and 2(b) for L/H=5.0 and L/H=1.5, respectively. The following observations are presented.

The proposed model gives results that are in very good agreement with Wood's exact results for both L/H=5.0 and L/H=1.5. The approximation of the proposed model works even better for a short backfill (L/H=1.5) than for a long backfill (L/H=5.0). Usually this model gives total force slightly less than the exact total force.

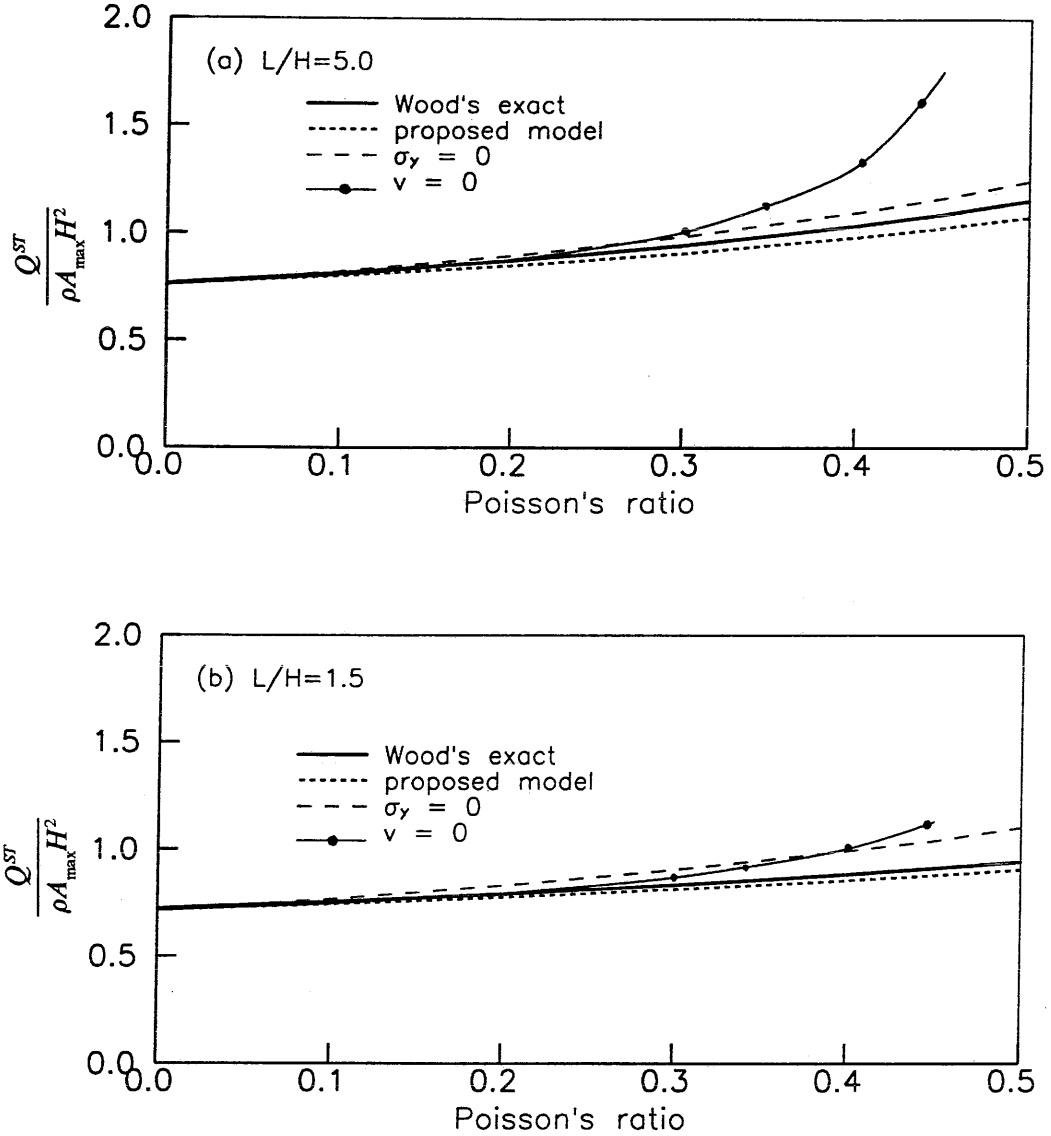

Fig. 2 Comparison of the Accuracy of Approximate Solutions for Rigid-Wall Systems (a) L/H=5.0 (b) L/H=1.5

The $\sigma_y = 0$ model yields results that are in very good agreement with the exact results for L/H=5.0. For wall-soil systems with L/H=5.0, the accuracy of the $\sigma_y = 0$ model is comparable to that of the proposed model. The difference between the two models is that the $\sigma_y = 0$ model overestimates the response but the proposed model underestimates the response slightly.

However for L/H=1.5, the $\sigma_y = 0$ model does not give as good results as the proposed model does. The solutions from the proposed model are much closer to the exact solutions than those from the $\sigma_y = 0$ model. The $\sigma_y = 0$ model may overestimate the total force by about 18%. The proposed model underestimates the total force by 4%.

When the v = 0 model is applied, the accuracy of the solution is very good provided Poisson's ration $\mu < 0.3$. As μ exceeds 0.3, the solutions start to deviate from the exact solutions. For L/H=5.0, the accuracy of the solution from the v = 0 model becomes unacceptable as $\mu > 0.4$.

The studies presented conclude that the proposed model gives the best approximation to solutions for the rigid-wall systems with infinite backfills and finite backfills. Therefore, the proposed model with $\theta = \beta = 2/(1 - \mu)$ is used for all further studies presented in this paper.

Static Thrust and L/H Ratio

Using the proposed model, the relationship between the static thrusts and the L/H ratios is evaluated and presented in Figure 3 for Poisson's ratio $\mu = 0.3$, 0.4 and 0.5. The static thrust plotted in Figure 3 are found to be independent of the shear modulus G of the backfill. The total thrusts increase with the increase of L/H ratio, but they approach steady values for L/H > 4. For L/H=5.0 and $\mu = 0.4$, the static thrust under 1-g static horizontal force (A_{max} = 9.81 m/sec^2) is estimated to be $1.0\,\gamma\,H^2$. For a 10 m high wall and a backfill with a unit weight γ = 19.6 kN/m^3, the static thrust is calculated to be 1960 kN for per unit wide wall. For values of μ other than 0.3, 0.4 and 0.5, the 1-g static thrusts can easily be obtained using Eq. (21).

The heights of the resultant static thrust due to the uniform horizontal body force are computed as functions of L/H ratios for μ = 0.3, 0.4 and 0.5. The heights do not change as μ varies at 0.3, 0.4 and 0.5, and they remain constant at 0.6H above the base of the wall when L/H is greater than 1.0.

FINITE ELEMENT SOLUTIONS FOR NONHOMOGENEOUS SOIL BACKFILLS

The nonhomogeneous soil backfills are modelled using the finite element method of analysis. A 6-node finite element which has 6 horizontal displacement variables is constructed to model the response of a soil element with a dimension of a by b. The composition of the finite element is shown in Figure 4. This finite element gives a quadratic variation of displacement u in the horizontal x direction and a linear variation in the vertical y direction. The detailed expressions of the shape functions N_i for this element are given in Wu (1994). The element stiffness matrix $[K]_{elem}$ is found from Eq. (1) using Galerkin's general procedure of weighted residuals.

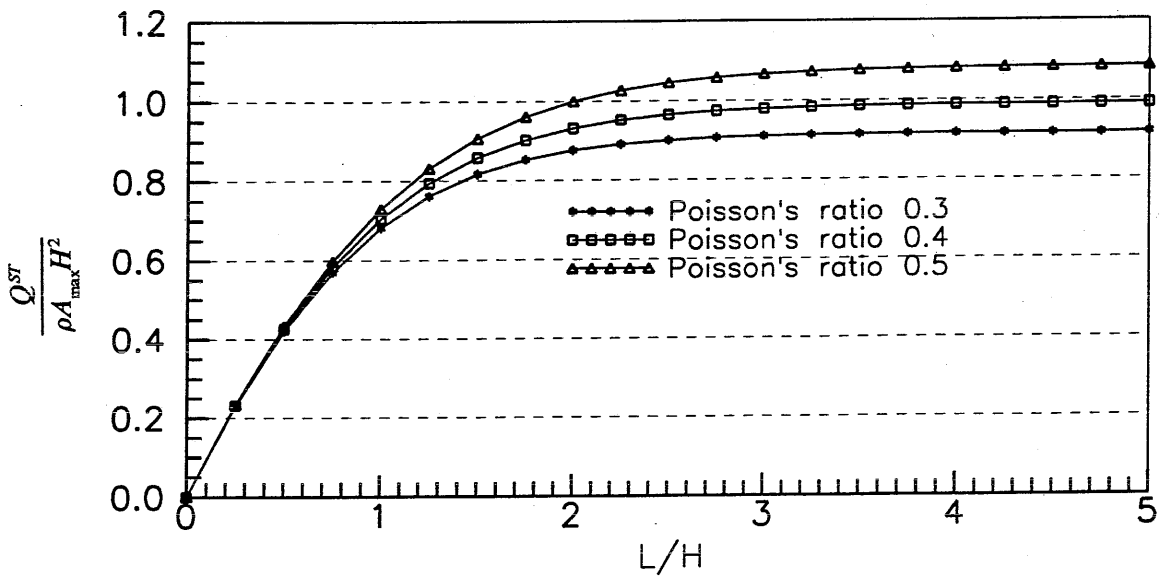

Fig. 3 Variation of Static Thrust with L/H Ratio for μ= 0.3, 0.4 and 0.5

$$[K]_{elem} = \int_0^a \int_0^b [G\frac{\partial N_i}{\partial y}\cdot\frac{\partial N_j}{\partial y} + \theta G\frac{\partial N_i}{\partial x}\cdot\frac{\partial N_j}{\partial x}]\, dx\cdot dy \qquad (22)$$

The diagonal terms of the diagonal mass matrix of the element is found to be

$$[M]_{elem} = \frac{\rho ab}{12}\{1,\ 1,\ 1,\ 1,\ 4,\ 4\} \qquad (23)$$

The element stiffness and mass matrices given in Eq. (22) and (23) are then applied to each element in the system. The global stiffness matrix [K] and the mass matrix [M] are assembled accordingly. The equations of motion are written in matrix form as

$$[M]\{\ddot{u}\} + [C]\{\dot{u}\} + [K]\{u\} = -[M]\{I\}\ddot{u}_b(t) \qquad (24)$$

where [C] is the damping matrix, and {I} is a column vector of 1.

The natural frequencies of the wall-soil system are determined by analyzing the eigen values of

the system. The damping matrix of each finite element is obtained according to the desired degree of damping of the element. In this manner the damping matrix [C] is evaluated.

The finite element theory has been verified against the analytical solutions using a homogenous soil backfill (Wu, 1994). Therefore the finite element method is considered to be a reliable tool for obtaining dynamic soil pressures for nonhomogeneous soil backfills. The finite element mesh used in the analysis is shown in Figure 5.

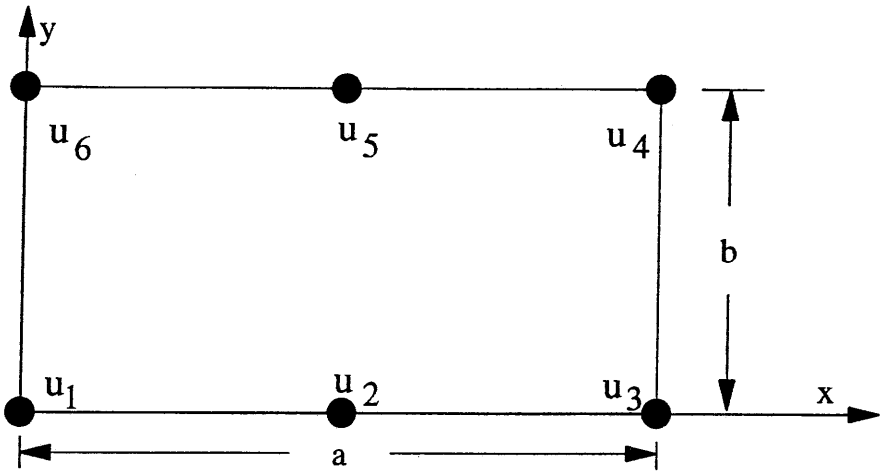

Fig. 4 The composition of the 6-node finite element

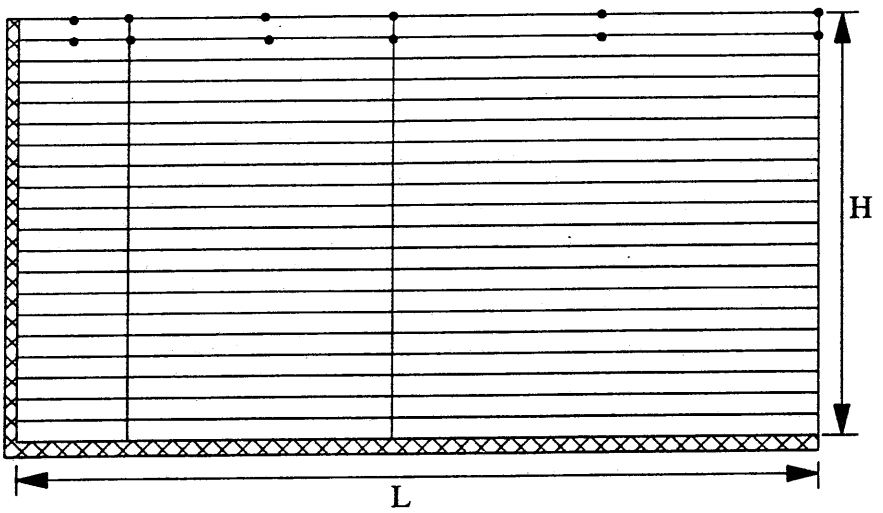

Fig. 5 The finite element mesh grid used in the analysis of nonhomogeneous soil backfills

RESULTS OF ANALYSES

The dynamic thrusts due to three types of soil profile namely, uniform G, parabolic G and linear G, have been investigated. The soil profiles of uniform G represent the homogeneous soil backfills with constant shear moduli G with depth. The soil profiles of parabolic G represent nonhomogeneous soil backfills with parabolic variation of shear moduli G with depth, and the linear G represents a linear variation of shear moduli G with depth. For the latter two cases the shear moduli G are assumed to vary from zero at the ground surface to G_{soil} at the bottom of the soil profile as shown in Figure 6. For all analyses presented, a Poisson's ratio of $\mu = 0.4$ and a damping ratio $\lambda = 10\%$ are used.

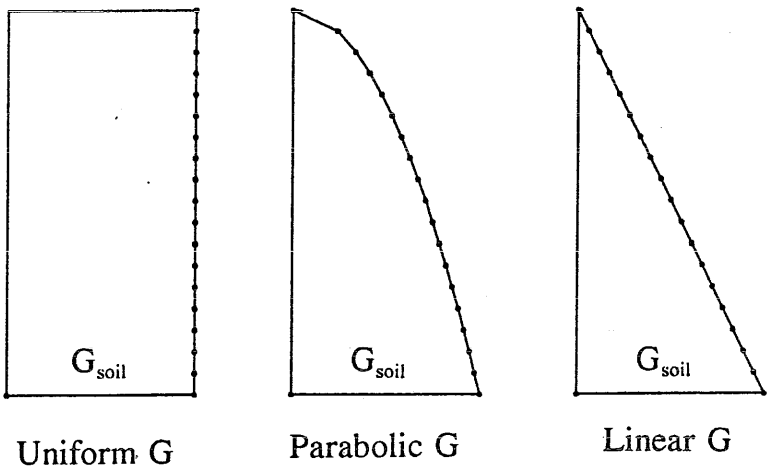

Fig. 6 Three Types of Soil Profile Representing the Backfills

Harmonic Base Excitation $\ddot{u}_b(t) = A_{max}\, e^{i\omega t}$

The peak dynamic thrusts at a steady state for various combinations of L/H and soil profile are presented in Figure 7. The normalized thrust ratios ($Q/\rho H^2 A_{max}$) are shown as functions of frequency ratios (ω/ω_{11}), in which ω represents the angular frequency of the excitation and ω_{11} represents the fundamental angular frequency of the wall-soil system. The values of ω_{11} are determined using Eq.(10) for homogeneous soil backfills, and they are computed from an eigen-value analysis using the finite element method for a nonhomogeneous soil backfill.

For backfills of uniform G, the static thrusts corresponding to infinitely low excitation frequency ω are $1.0\rho H^2 A_{max}$ for L/H=5.0 and $0.86\rho H^2 A_{max}$ for L/H=1.5. The dynamic thrusts increase as the excitation frequency approaches the fundamental frequency of the wall-soil system. At resonant conditions, the peak dynamic thrusts are $2.4\rho H^2 A_{max}$ for L/H=5.0 and $3.0\rho H^2 A_{max}$ for

L/H=1.5. The corresponding dynamic amplification factors are 2.4 for L/H=5.0 and 3.5 for L/H=1.5. The results suggest that the dynamic amplification for wall-soil systems with finite backfills is larger than that for wall-soil systems with semi-infinite backfills.

For nonhomogeneous backfills with L/H=5.0, the static thrust are about $0.82\rho H^2 A_{max}$ for backfills of parabolic G and $0.71\rho H^2 A_{max}$ for backfills of linear G. At resonance the peak dynamic thrusts are $1.87\rho H^2 A_{max}$ for backfills of parabolic G and $1.56\rho H^2 A_{max}$ for backfills of linear G. The corresponding dynamic amplification factors are 2.3 and 2.2, respectively.

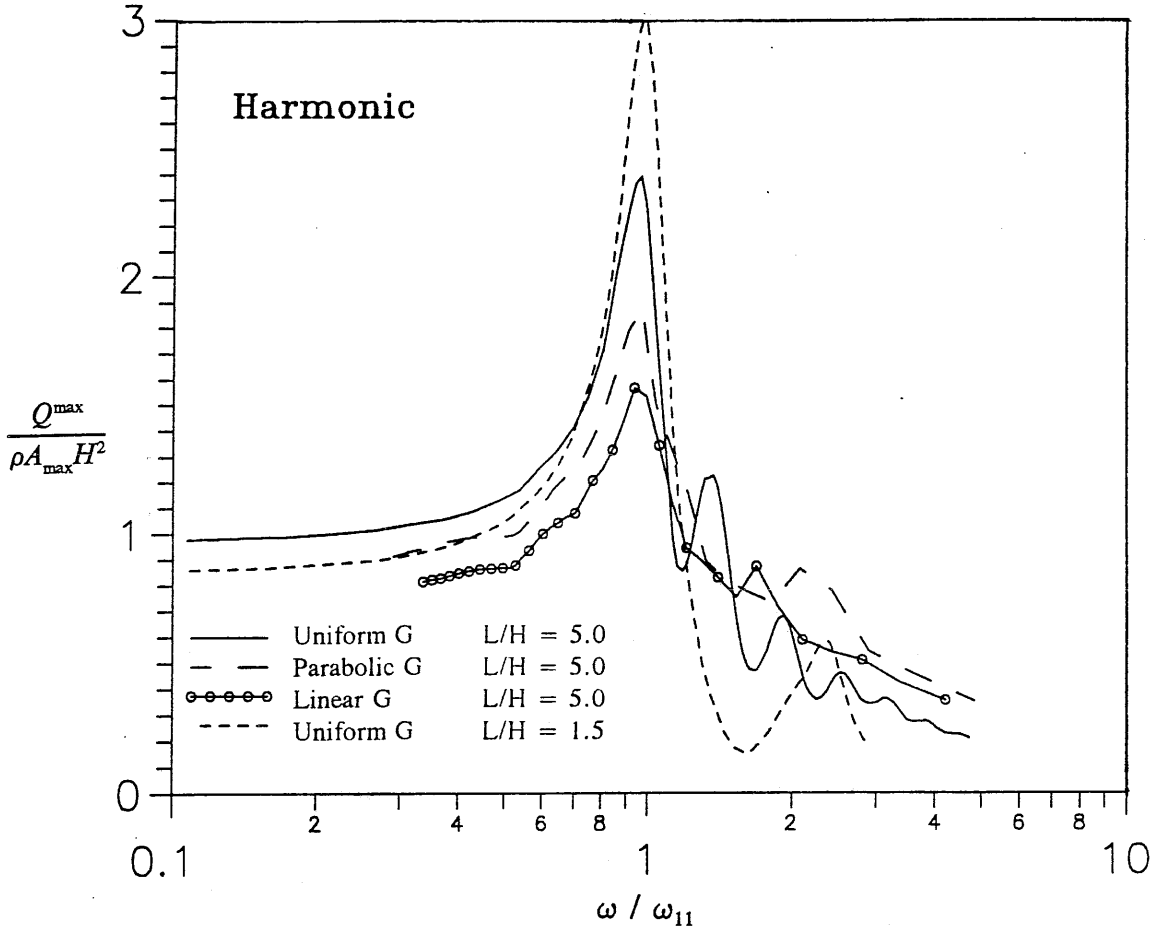

Fig. 7 Peak Dynamic Thrusts at Steady State under Harmonic Excitation ($\lambda = 10\%$, $\mu = 0.40$)

Seismic Base Excitation

Seismic base motions are represented by 10 accelerations recorded in the past earthquake events. The time histories of the input accelerations are shown in Fig. 8. These earthquake accelerations are selected to cover a variety range of excitation frequencies. Descriptions of these

accelerograms are given in Table 1. The angular frequencies of these accelerograms are determined by the frequencies corresponding to peak spectral accelerations and are given in Table 1.

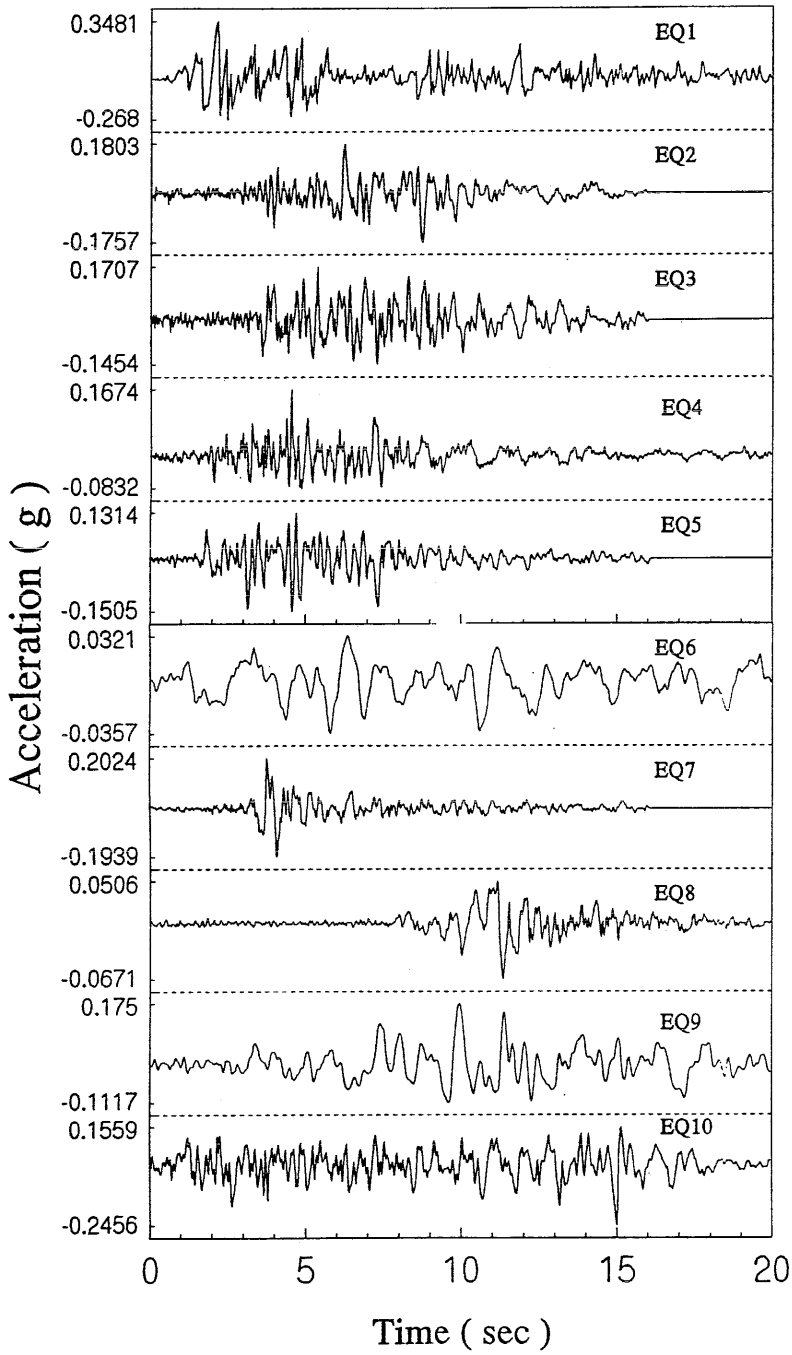

Fig. 8. The Time Histories of 10 Seismic Accelerograms Used in the Analyses

Table 1. Characteristics of Seismic Accelerograms Used in the Analyses

Name of Accelerograms	Descriptions
EQ1	El Centro Earthquake, 1940; Station: Imperial Valley, CA; Components: S00E; Peak: 0.348g; ω = 11.64 rad/sec
EQ2	San Fernando Earthquake, 1971; Station: Griffith Park, L.A.; Component: S00E; Peak 0.180g; ω = 25.13 rad/sec
EQ3	San Fernando Earthquake, 1971; Station: Griffith Park, L.A.; Component: S90E; Peak 0.171g; ω = 25.13 rad/sec
EQ4	San Fernando Earthquake, 1971; Station: Lankershim St., CA; Component: S00E; Peak 0.167g; ω = 31.4 rad/sec
EQ5	San Fernando Earthquake, 1971; Station: Lankershim St., CA; Component: S90E; Peak 0.151g; ω = 25.13 rad/sec
EQ6	Partial segment of a rock motion recorded during the 1985 Mexico City Earthquake; Peak 0.0357g; ω = 7.0 rad/sec
EQ7	Monte Negro Earthquake, 1979; Station: Bar, City Hall; Component: S00E; Peak 0.202g; ω = 12.57 rad/sec
EQ8	Loma Prieta Earthquake, 1989; Station: Yerba Buena Island, CA; Component: S90E; Peak 0.0671g; ω = 10.13 rad/sec
EQ9	Loma Prieta Earthquake, 1989; Station: Stanford University, CA; Component: S00E; Peak 0.175g; ω = 10.47 rad/sec
EQ10	artificial accelerogram; modified from a recorded accelerogram of the Puget Sound Earthquake, 1949; Peak 0.246g; ω = 18.0 rad/sec

Dynamic peak thrusts and heights of thrust are obtained using the analytical and finite element solutions presented in the earlier sections. The peak dynamic thrusts are computed for three types of soil profile (Fig. 6) under earthquake loads represented by the ten accelerograms. For each type of soil profile, the shear moduli G of the soil are proportionally reduced 25 times to simulate a variety range of soil stiffness. The reduction of soil stiffness results in decrease of the fundamental frequency ω_{11} of the wall-soil system as shown in Fig. 9. Corresponding to each soil stiffness analyses are conducted using the ten accelerograms as input motions.

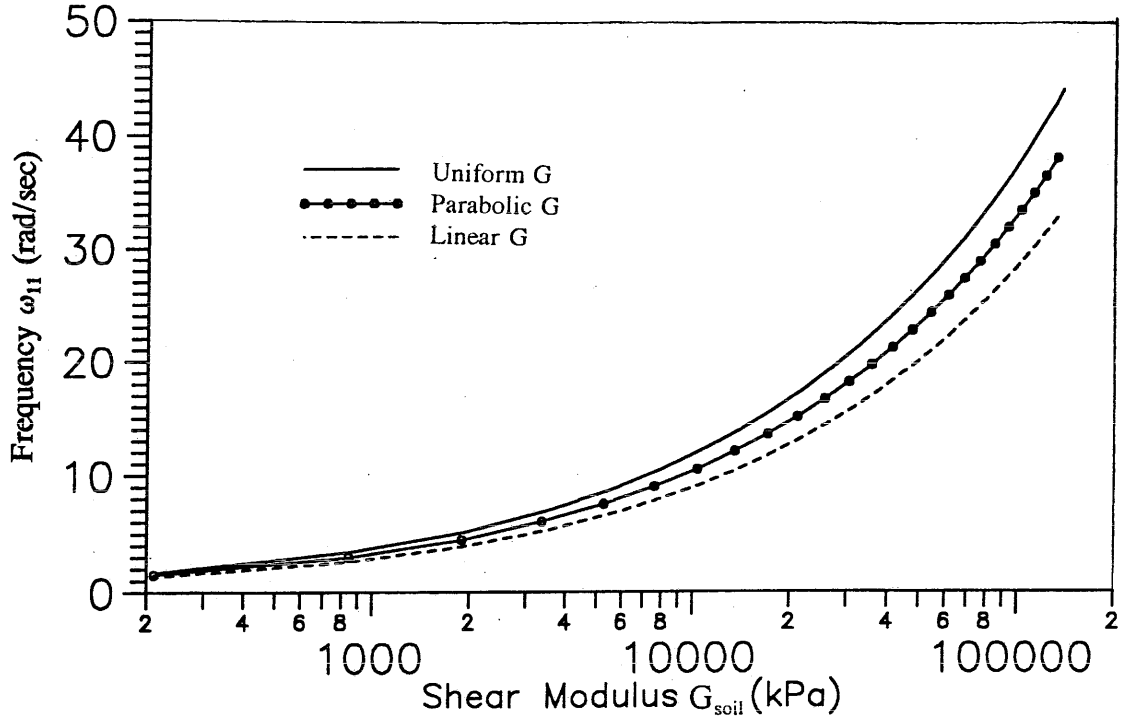

Fig. 9 Variations of the fundamental angular frequencies ω_{11} of the wall-soil systems with soil stiffness (wall height H=10.0 m; soil density ρ=2.0; soil Poisson's ratio μ=0.4, L/H=5.0)

Therefore, 250 combinations of accelerogram and shear modulus G are examined for each type of soil profile.

The computed peak seismic thrust ratios $Q^{max}/\rho A_{max}H^2$ are shown in Figs. 10 through 12 for the soil profile of uniform G, parabolic G and linear G, respectively. These results are obtained for rigid walls retaining semi-infinite backfills, which are represented by L/H = 5.0. Analyses are also conducted to determine the seismic thrusts against rigid walls retaining backfills of finite length, which are represented by L/H = 1.5. The peak seismic thrust ratios are shown in Fig. 13 for the soil profile of parabolic G. The upper bound envelopes of these peak seismic thrust ratios are shown in Fig. 14. The heights of thrust are fairly constant over the entire range of ω/ω_{11} ratio, and they are shown in Fig. 15. The following observations are made from these results:

- Under seismic loads the upper bound peak seismic thrusts against walls with semi-infinite backfills could be as high as $1.7\rho H^2A_{max}$ for a uniform soil profile, $1.35\rho H^2A_{max}$ for a parabolic soil profile, and $1.15\rho H^2A_{max}$ for a linear soil profile.
- The peak seismic thrust decreases significantly as the frequency ratio ω/ω_{11} is greater than two. This result strongly indicates that the seismic thrust ratios $Q^{max}/\rho H^2A_{max}$ against

a higher wall of a soft backfill may be much less than that against a shorter wall of a stiff backfill.

- The wall-soil system with more uniform backfill tends to generate larger seismic thrust against the wall.
- Amplification of seismic thrusts at resonance are much larger for soils contained by two narrow walls (L/H =1.5) than for semi-infinite soils (L/H=5.0). The peak seismic thrust against walls with soils of L/H=1.5 reaches $1.7\rho H^2 A_{max}$ because of this amplification.
- The heights of seismic thrust are suggested to be at 0.64H above the base of the wall for the soil profile of uniform G. However the heights decrease to 0.5H for soil of linear G (Fig. 15).

The results of dynamic thrusts are also summarized in Table 2. The seismic thrusts computed using the Mononobe - Okabe method are given in the same table. The M-O method gives total forces acting on the wall using the conditions of limit equilibrium. The total forces are computed using the coefficient K_{AE} for seismic active pressures and the coefficient K_{PE} for seismic passive pressures (Seed and Whitman, 1970). The seismic thrusts in the M - O method are found by subtracting the total forces by the earth pressures at rest. A lateral earth pressure coefficient $K_0 = 1 - \sin\phi$ is used for this purpose.

Table 2. Summary of Peak Dynamic Thrust Ratios α (Dynamic Thrust = $\alpha\rho A_{max}H^2$)

	Static Solution	Harmonic loads	Seismic Loads	Mononobe - Okabe Seismic Pressures (1)	
				A_{max} =0.3g	A_{max}=0.5g
Uniform G L/H = 5.0	1.00	2.40	1.70	K_{AE} = 0.478 K_{PE} = 3.063	K_{AE} = 0.716 K_{PE} = 2.545
Parabolic G L/H=5.0	0.82	1.87	1.35	Seismic thrust ratios: Active α = 0.08 Passive α = 4.39	Seismic thrust ratios: Active α = 0.29 Passive α = 2.12
Linear G L/H=5.0	0.71	1.56	1.15		
Uniform G L/H=1.5	0.86	3.00			
Parabolic G L/H=1.5	0.82		1.70		

(1) In M - O method, the wall is assumed to be vertical and frictionless, and the friction angle of the soil is ϕ = 35°.

It can be seen that the peak seismic thrusts against rigid walls are generally much less than the seismic passive pressures computed by using the M - O method. But they are much larger than the seismic active earth pressures. This is especially true under small accelerations. Under strong shaking, the upper bound seismic thrusts against rigid walls are closer to the seismic passive pressures. This does not include the effect of soil nonlinearity under strong shaking which may reduce the frequency of the wall -soil system and therefore reduce the peak seismic thrusts.

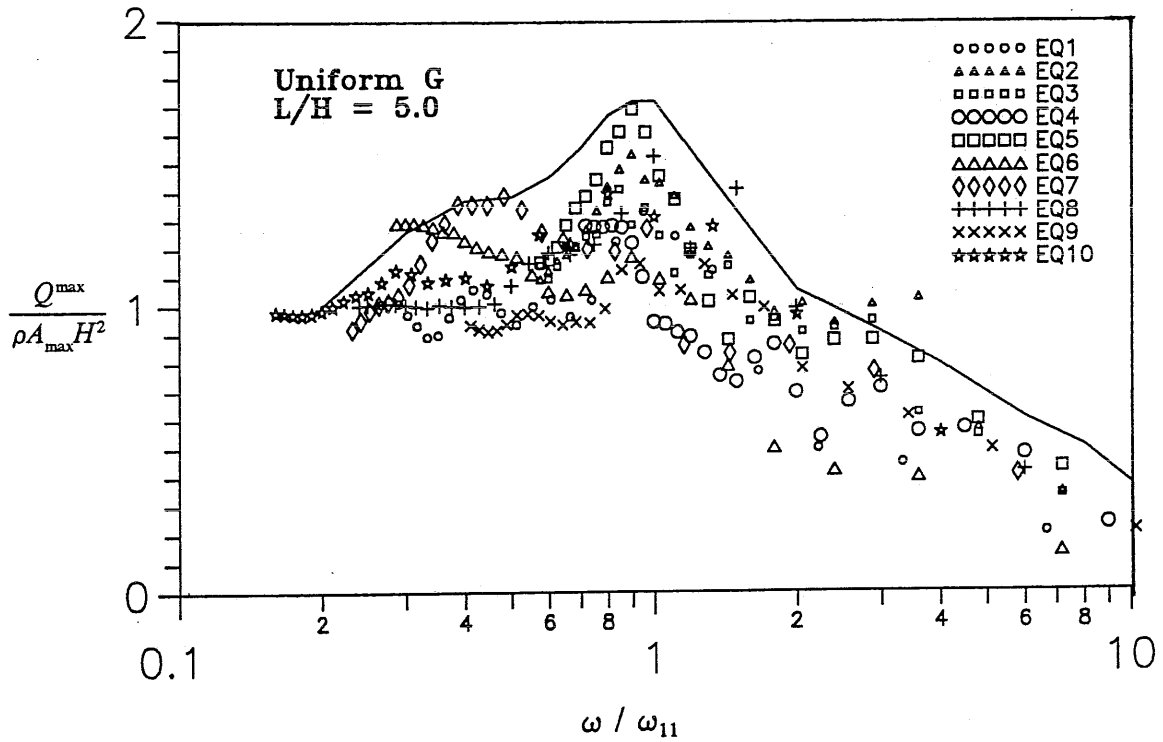

Fig. 10. Peak Seismic Thrusts for Soil Profiles of Uniform G (L/H = 5.0, λ = 10%, μ = 0.40)

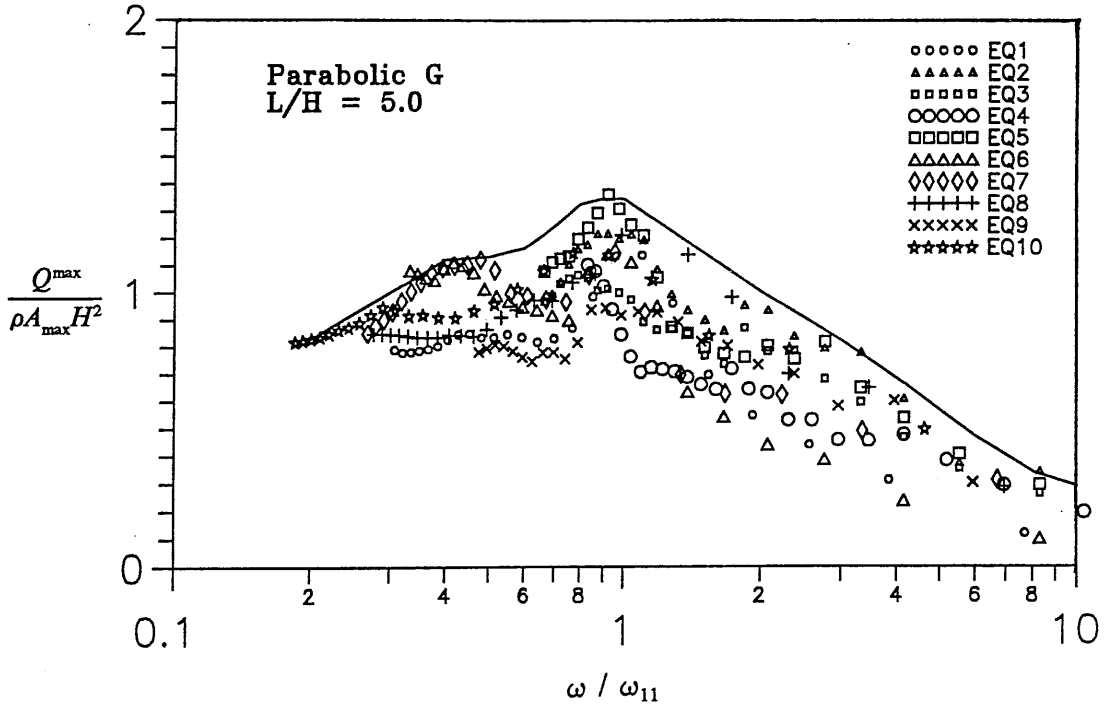

Fig. 11. Peak Seismic Thrusts for Soil Profiles of Parabolic G (L/H=5.0, λ = 10%, μ = 0.40)

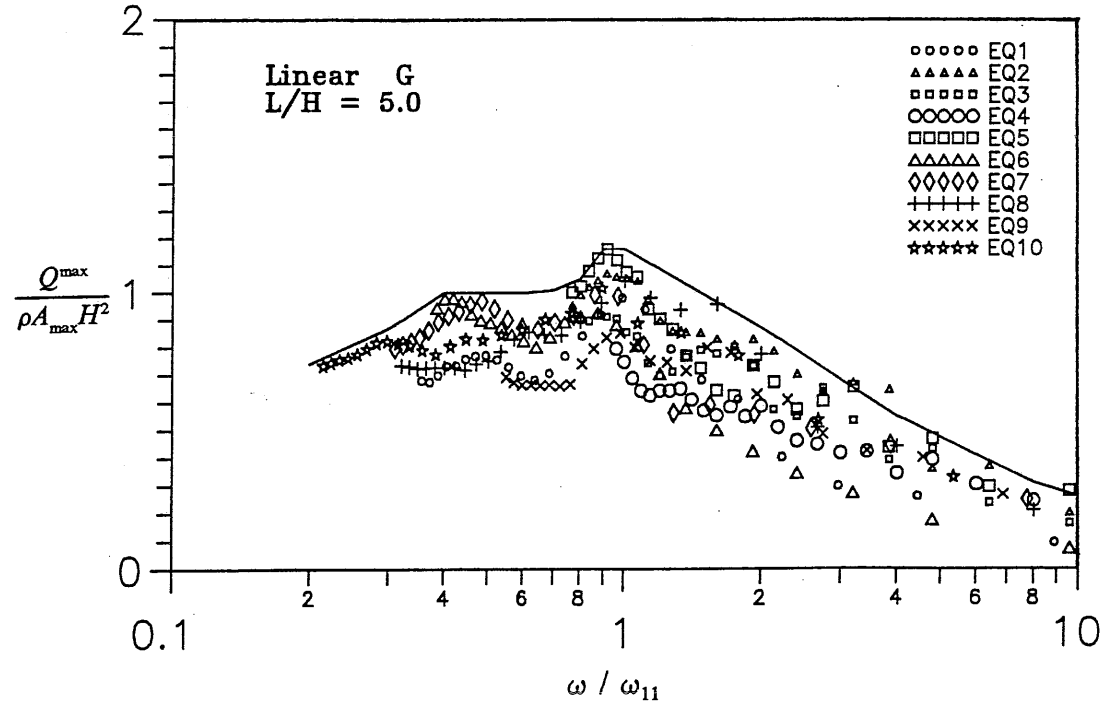

Fig. 12. Peak Seismic Thrusts for Soil Profiles of Linear G (L/H = 5.0, λ = 10%, μ = 0.40)

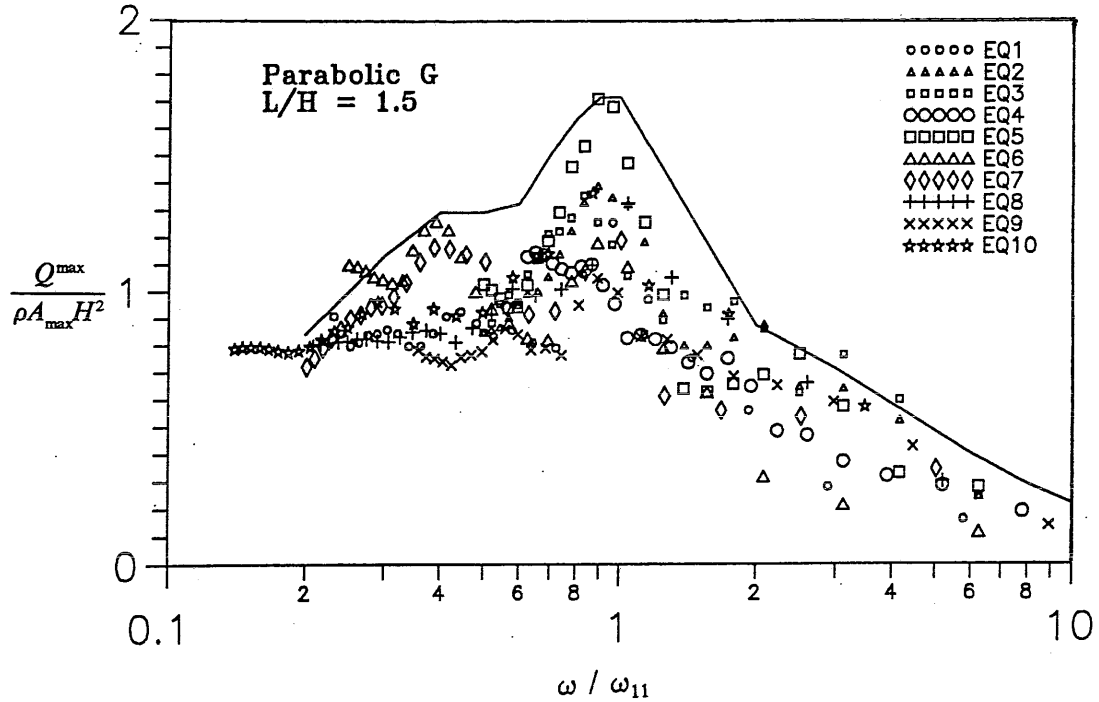

Fig. 13. Peak Seismic Thrusts for Soil Profiles of Parabolic G (L/H=1.5, λ = 10%, μ = 0.40)

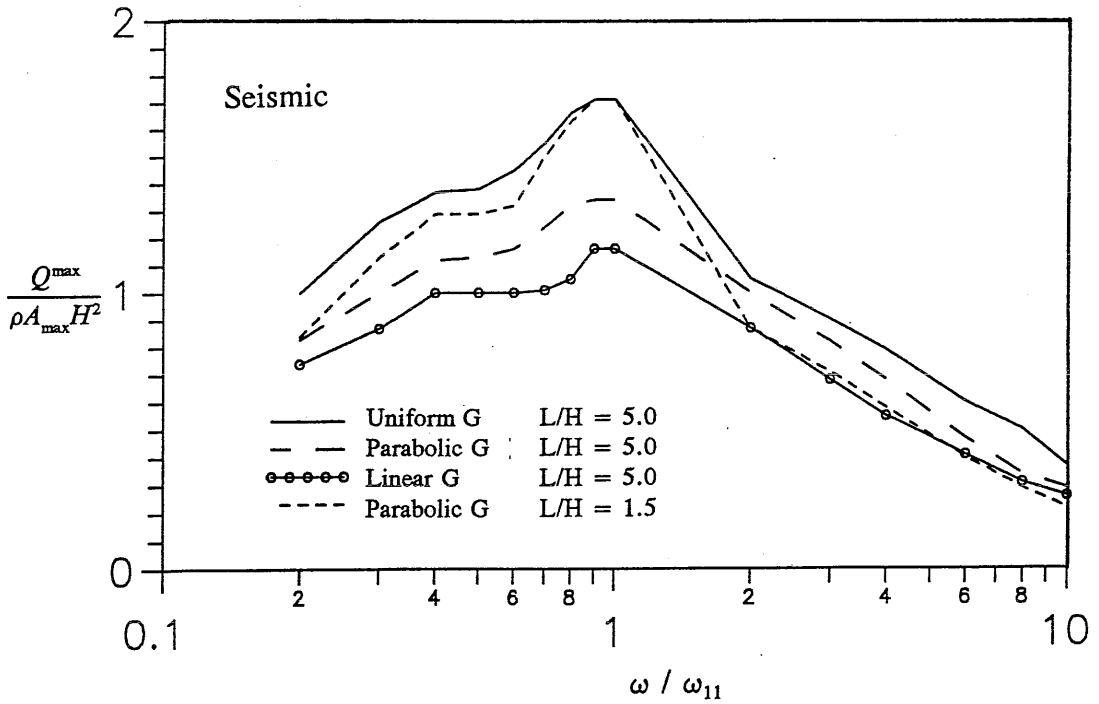

Fig. 14. Upper Bound Envelopes of Peak Seismic Thrusts (λ = 10%, μ = 0.40)

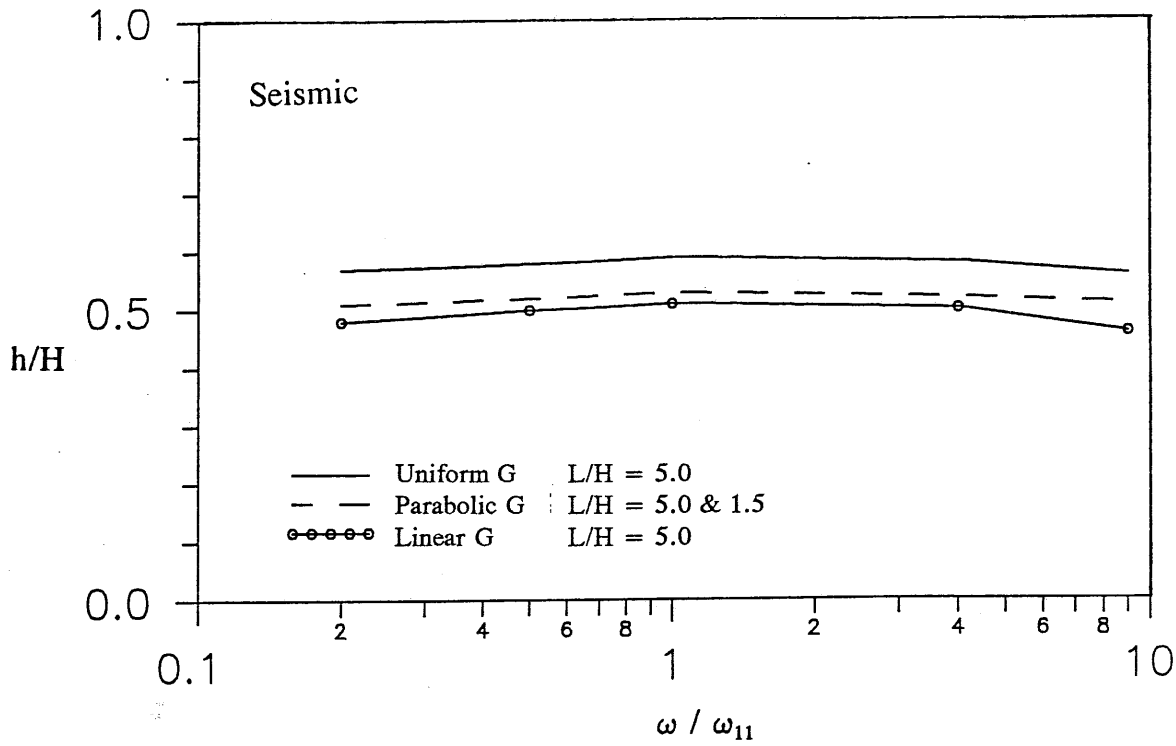

Fig. 15. Heights of Seismic Thrusts for the Three Soil Profiles (λ = 10%, μ = 0.40)

CONCLUSIONS AND DISCUSSION

An approximate method for determining the dynamic thrusts against rigid walls subjected to horizontal dynamic loads has been presented. Analytical solutions have been presented for computing dynamic thrusts against rigid walls with uniform backfills. The solutions given by the proposed method are in good agreement with Wood's rigorous solutions.

Peak dynamic thrusts against rigid walls have been evaluated using the proposed method. Results of analysis show that the peak seismic thrusts Q^{max} could be as high as $1.7\rho A_{max}H^2$ with A_{max} being the peak horizontal acceleration. Results also show the variations of Q^{max} with the frequency of the input excitation and the frequency of the wall-soil system. Upper bound envelopes of these seismic thrusts have been constructed based on the results of these analyses.

Although the method has been applied for analysis of wall-soil systems under linear elastic conditions with a constant damping ratio λ=10%, the results of these analyses may be extended to nonlinear wall-soil systems typically under strong shaking. This application requires

estimating the reduction of shear modulus of the entire soil profile under such a strong shaking. The seismic thrust against the wall may then be estimated using the fundamental frequency of the wall-soil system ω_{11} corresponding to the reduced shear modulus.

ACKNOWLEDGEMENT

The postgraduate fellowship (1992 - 1994) awarded by the Natural Sciences and Engineering Research Council of Canada is acknowledged. The support from Professor W.D.Liam Finn of the University of British Columbia is greatly appreciated.

REFERENCES:

Matuo, H., and Ohara, S. 1960. Lateral Earthquake Pressure and Stability of Quay Walls During Earthquakes. Proceedings of the Second World Conference on Earthquake Engineering, Vol. 2.

Mononobe, N., and Matuo, H. 1929. On the Determination of Earth Pressure during Earthquakes. Proceedings of World Engineering Conference, Vol 9.

Okabe, S. 1926. General Theory of Earth Pressure. Journal of Japanese Society of Civil Engineers, Vol. 12, No. 1.

Scott, R.F. 1973. Earthquake-Induced Earth Pressures on Retaining Walls. Proceedings of the Fifth World Conference on Earthquake Engineering, Rome, Italy.

Seed, H. B., and Whitman, R. V. 1970. Design of Earth Retaining Structures for Dynamic Loads. Proceedings of ASCE Special Conference on Lateral Stresses, Ground Displacement and Earth Retaining Structure, Ithaca, N.Y., pp. 103 - 147.

Veletsos, A.S. and Younan, A.H. 1994. Dynamic Soil Pressures on Rigid Vertical Walls. International Journal of Earthquake Engineering and Structural Dynamics, **23:** 275-301.

Wood, J. H. 1973. Earthquake-Induced Soil Pressures on Structures. Ph.D thesis, the California Institute of Technology, Pasadena, California, USA.

Wu, Guoxi 1994. Dynamic Soil-Structure Interaction: Pile Foundations and Retaining Structures. Ph.D. thesis, Department of Civil Engineering, the University of British Columbia, B.C., Canada.